

FY2018 Progress Report To:
the
Japan Aerospace Exploration Agency

**Validation of global water and energy
balance monitoring in the Australian
Murray-Darling Basin using GCOM-W1
data**

Specification No: **JX-PSPC-500191**; Contract No: **17RSTK005381**

Investigators: Jeffrey Walker (RA1W108), Jason Beringer, Christoph Rüdiger,
Edoardo Daly

Contributors: Ying Gao, Mei Sun Yee, Kiri Manson

March 2019



Executive Summary

This report presents the research activities and outcomes for the project ‘Validation of global water and energy balance monitoring in the Australian Murray-Darling Basin using GCOM-W1 data’ during JFY 2018. The research activities aims to continue operating the JAXA flux tower within the core validation site located in Yanco, New South Wales, Australia, and provide spatially distributed soil moisture data from across an AMSR2 sized footprint. Importantly, this project will also make significant independent and collaborative contributions to validation of:

- i) the low resolution AMSR2 soil moisture products;
- ii) a high resolution downscaled AMSR2 soil moisture product; and
- iii) land surface model simulations of soil moisture and latent/sensible heat.

Due to delay in obtaining the land surface model simulated soil moisture and flux data, the research work during JFY 2018 mainly focused on the first and second targets.

Similar to JFY 2017, results from 2018 indicated that the AMSR2 L3 soil moisture product match with the JAXA tower and in-situ station measurements relatively well during the dry season when soil moisture is smaller than $0.1 \text{ m}^3/\text{m}^3$. However, during the wet season (soil moisture $\sim 0.1\text{-}0.5 \text{ m}^3/\text{m}^3$), the AMSR2 product tends to underestimate the condition by around $0.1\text{-}0.3 \text{ m}^3/\text{m}^3$ compared with the peak soil moisture values. Nevertheless, the underestimation status is better than the wetter

years 2015-2016. It is suggested that the AMSR2 L3 soil moisture algorithm needs to be improved in the future.

The downscaling schemes and the soil moisture retrieval algorithms were also presented in this report. Results show the relationship between downscaled C-band TB and airborne L-band TB observations align very well with the low-resolution SMAP L-band TB against AMSR2 C-band TB.

Table of Contents

Executive Summary.....	1
Table of Contents	3
List of Figures	5
Chapter 1: Introduction.....	1
Chapter 2: Site Description	3
2.1 The Murrumbidgee Catchment.....	3
2.2 The Yanco site.....	5
Chapter 3: Flux Tower Maintenance for JFY2018.....	8
Chapter 4: Data Sets	12
4.1 Flux tower data updates for JFY2018	12
4.2 OzNet monitoring network data	17
4.3 Airborne brightness temperature data.....	19
4.4 AMSR2 Level 3 soil moisture product	22
Chapter 5: Validation of AMSR-2 Level 3 soil moisture products.....	25
5.1 Time series.....	25
5.2 Scatter plots	28

Chapter 6: Downscaling of low-resolution C-band Brightness Temperature from AMSR2	32
6.1 The SFIM downscaling methodology	32
6.2 Input: AMSE-2 C-band and Ka-band TB products	34
6.3 Output: Downscaled C-band TB product	37
Chapter 7: Summary and Conclusion	42
References	43

List of Figures

Figure 1: Location of the Yanco core validation site within the Murrumbidgee Catchment. Also shown is the location of the Murrumbidgee Catchment within the Murray-Darling Basin (inset) and the locations of sparse network soil moisture stations.....	4
Figure 2: Locations of the JAXA flux station, weather station and soil moisture monitoring stations within the Yanco core validation site. Also shown are the YA and YB focus areas with intensive soil moisture stations, and the locations of intensive ground sampling areas.	6
Figure 3: Calibration of the Open Path CO ₂ /H ₂ O Gas Analyzer (LI-7500A).	9
Figure 4: Monash technician climbing the tower to remove sensor for calibration....	9
Figure 5: TRIME-PICO32, 10 cm soil moisture sensor (green) broken since Nov 2016.	10
Figure 6: Campbell Met One 034B Windset; 8m (green) broken since late July 2018; 2m (pink) broken from July to August 2018 and from mid-December 2018 till present.....	10
Figure 7: Mislocated Humidity and Temperature Probe (HMP 155) inside the Vaisala Weather Transmitter (WXT530), to be re-installed on to the tower at 16m height.....	11
Figure 8: JAXA data download interface on http://www.oznet.org.au/mdbdata/mdbdata.html	12

Figure 9: Soil moisture data at 3cm, 10cm, 15cm, 45cm and 75cm from the tower. 13

Figure 10: Soil temperature data at 3cm, 10cm, 15cm, 45cm and 75cm from the tower..... 13

Figure 11: Latent/sensible heat and water vapor due to latent/sensible heat from the tower. 14

Figure 12: Wind speed at 2m, 4m, 8m and 16m measured from the tower. 14

Figure 13: Real-time tower data interface on <http://www.science.uwa.edu.au/centres/land/yanco>. 15

Figure 14: Examples of real-time figures for flux data available on the above website..... 16

Figure 15: Example of soil moisture and temperature collected from YA5 from March 2018 to February 2019. 18

Figure 16: Study area and airborne monitoring are during SMAPEX-5 19

Figure 17: Airborne brightness temperature at V-polarization from SMAPEX-4 at Yanco area. Title of each subplot indicates flight date with the format of YYYYMMDD..... 20

Figure 18: Airborne brightness temperature at V-polarization from SMAPEX-5 at Yanco area. Title of each subplot indicates flight date with the format of YYYYMMDD..... 21

Figure 19: Location of the 10-km and 25-km AMSR2 L3 SMC pixel, SMAP 36-km pixel with respect to the flux tower location..... 22

Figure 20: Time series of the AMSR2 L3 10-km and 25-km soil moisture in the Yanco site. 23

Figure 21: Box plot of the AMSR2 L3 10-km and 25-km soil moisture in the Yanco site. 23

Figure 22: Time series plot of AMSR2 L3 10- and 25-km soil moisture product against JAXA flux tower soil moisture measured at 3-cm depth. 26

Figure 23: Scatter plots of AMSR2 SM (10-km) against soil moisture from the tower, SMAP observations, YA5 station and YB7a station. 29

Figure 24: Scatter plots of tower soil moisture against AMSR2 SM (10-km), SMAP SM (36-km), YA5 and YB7a station soil moisture. 30

Figure 25: Comparison of AMSR2 L3 SM validation in 2017-2018 against 2015-2016. 31

Figure 26: A schematic plan for AMSR2 soil moisture downscaling and validation procedures. 33

Figure 27: AMSR2 L1B map of C-band and Ka-band TB (Ascending) over SMAPEX-4. 35

Figure 28: AMSR2 L1B map of C-band and Ka-band TB map (Descending) over SMAPEX-4. 36

Figure 29: Linear regression between aggregated Ka-band and C-band brightness temperature at 50-km resolution. 38

Figure 30: Downscaled C-band TB at 10-km resolution during SMAPEX-4 (PM and AM); Airborne L-band TB measurements by PLMR at the same days (AM). 39

Figure 31: Correlation between C-band and L-band brightness temperature from satellite and airborne campaign measurements. 40

Chapter 1: Introduction

This report presents a range of research activities and outcomes of the project Validation of global water and energy balance monitoring in the Australian Murray-Darling Basin using GCOM-W1 data during JFY2018. The project seeks to continue operating the JAXA flux tower within the core validation site located in Yanco, New South Wales, and provide spatially distributed soil moisture data from across an AMSR2 sized footprint. Importantly, this project will also make significant independent and collaborative contributions to validation of: i) the low resolution AMSR2 soil moisture products; ii) a high resolution downscaled AMSR2 soil moisture product; and iii) land surface model simulations of soil moisture and latent/sensible heat.

During JFY2018, the main research activities include regular site visit and maintenance of the JAXA flux tower, data downloading and processing. The processed soil moisture data was used to validate the 10-km and 25-km resolution AMSR2 soil moisture products. On the other hand, the high-resolution Ka-band brightness temperature (TB) from AMSR2 was used to downscale the low-resolution C-band TB using the smoothing filter-based intensity modulation (SFIM) method. The relationship of the downscaled 10-km C-band data against L-band airborne measurement during the 2015 SMAPEX campaign was compared with the relationship of the 50-km C-band data against SMAP L-band observation to validate their consistency.

Due to the delay in obtaining land surface model simulation of soil moisture and latent/sensible heat data, validation of these against tower measurements will be moved into the research outcomes of the following year.

Chapter 2: Site Description

2.1 The Murrumbidgee Catchment

The Murrumbidgee catchment is located in southern NSW, Australia. It is bordered by the Great Dividing Range to the east, the Lachlan catchment to the north, and the Murray catchment to the south. The Murrumbidgee Catchment exhibits a significant spatial variability in climate, soil, vegetation and land cover because of its distinctive topography (Figure 1). Due to the diversity within this area, the large amount of complementary data from long-term monitoring sites, and past airborne field experiments, this region is an ideal test-bed for the comprehensive validation of satellite soil moisture from missions such as GCOM-W1 and is highly complementary to validation sites in Mongolia and Thailand. Moreover, considering the size of the satellite footprint, there are regions in the catchment that are relatively homogeneous in regard to climate, soil type, vegetation, and consequently radiometric response (Rüdiger et al., 2011) when compared to many other countries.

Temporal climatic variations of the catchment are primarily associated with elevation, varying from semi-arid in the west to temperate in the east. The total average annual rainfall for the entire Murrumbidgee River catchment is about 530 mm, with a mean annual precipitation of 300 mm in the west and about 1,900 mm towards the east in the Snowy Mountains. The actual evapotranspiration is equivalent to precipitation in the west but represents only half of the precipitation in the east. Long term averaged precipitation data for the Murrumbidgee

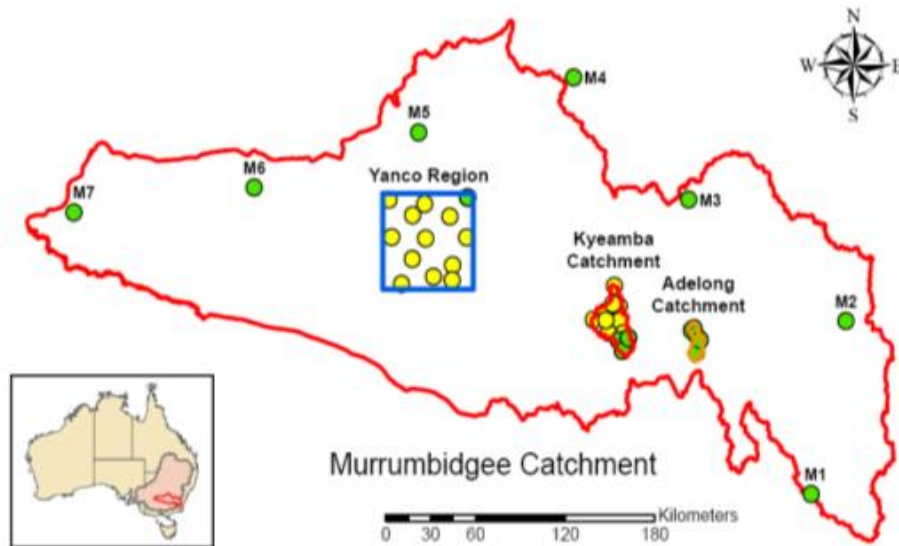


Figure 1: Location of the Yanco core validation site within the Murrumbidgee Catchment. Also shown is the location of the Murrumbidgee Catchment within the Murray-Darling Basin (inset) and the locations of sparse network soil moisture stations.

Catchment shows a relatively constant rate of rainfall across the year, with a slight increase in winter. The Murrumbidgee catchment is characterised by plains in the west with an elevation around 50 m, to steep mountainous regions towards the east with elevations more than 2,100 m in the Snowy Mountains. Soils in the Murrumbidgee Catchment vary from sand to clay, with the western plains being dominated by finer-textured soils and the eastern slopes being dominated by medium-to-coarse textured soils (McKenzie et al., 2000).

Land use in the catchment is predominantly agricultural with the exception of steeper parts, which are dominated by a mixture of native eucalypt forests and exotic forestry plantations. Agricultural land use varies greatly in intensity and includes pastoral, more intensive grazing, broad-acre cropping, and intensive agriculture in irrigation areas along the mid-lower Murrumbidgee. Grazing is predominant in the west and scattered in the east, whereas dryland cropping

dominates the mid Murrumbidgee catchment. Irrigation sites are mainly located in western part of the Yanco core validation site. The catchment is comprised of about 52% pasture, followed by about 21% arable and 18% silvicultural land use. The other land use types represent less than 9% of the total catchment area.

2.2 The Yanco site

The Yanco area is a 60 km x 60 km area located in the western plains of the Murrumbidgee Catchment where the topography is flat with very few geological outcroppings (Figure 2). Soil types are predominantly clays, red brown earths, transitional red brown earth, sands over clay, and deep sands. Approximately one-third of the core validation site is irrigated during summer when sufficient water is available. The Coleambally Irrigation Area (CIA) is a flat agricultural area of approximately 95,000 hectares that contains more than 500 farms. The principal summer crops grown in the CIA are rice, corn, and soybeans, while winter crops include wheat, barley, oats, and canola. Rice crops are usually flooded in November by about 30 cm of irrigation water.

A total of 24 surface soil moisture sites were installed in late 2009 to develop a nested soil moisture monitoring configuration for the SMAP mission at scales of approximately 3 km, 9 km and 36 km. These stations continuously monitor the soil moisture over the 0-5 cm layer with a Hydraprobe and soil temperature sensors (Unidata® 6507A/10) at 1, 2.5 and 5cm depths. The 24 sites are concentrated on two 9 km x 9 km focus areas (areas YA and YB), corresponding to two pixels of the SMAP grid at which the active passive soil moisture product (SMAP L3_SM_A/P product) was to be produced. Finally, 10 of the sites within areas YA and YB are concentrated on a further two 3 km x 3 km sub-areas (each) with at least 4 stations

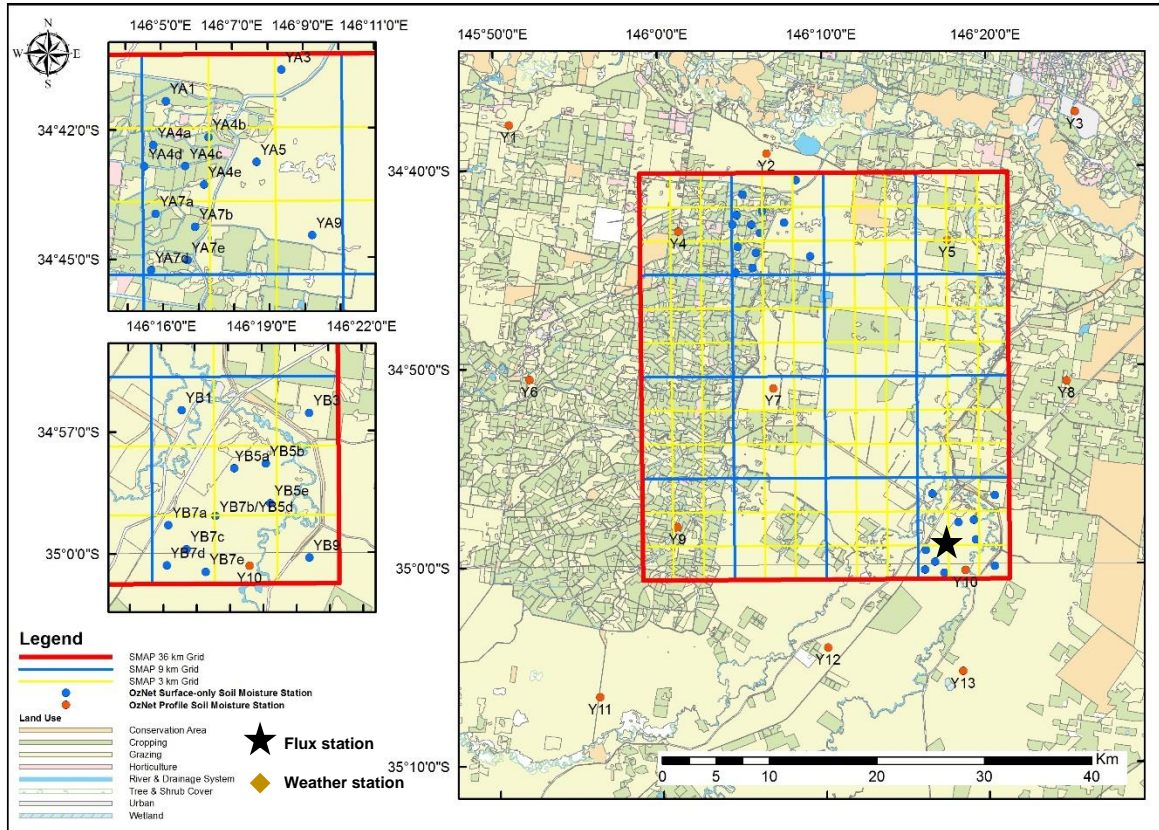


Figure 2: Locations of the JAXA flux station, weather station and soil moisture monitoring stations within the Yanco core validation site. Also shown are the YA and YB focus areas with intensive soil moisture stations, and the locations of intensive ground sampling areas.

measuring the distribution of soil moisture across each, corresponding to a total of four of the SMAP radar pixels (see Figure 2 for details of the YB area). Unfortunately, the SMAP radar failed shortly after commissioning. However, sentinel data are being used to replace the SMAP radar observations for locations such as the Murray Darling Basin.

This intensive network is also an ideal core validation site for AMSR2, as it i) monitors soil moisture across an AMSR2 sized pixel with approximately 30 stations, and ii) can be used to validate AMSR2 downscaling algorithms through the nested sampling design and supplementary intensive ground sampling activities that have

been undertaken. Moreover, extensive airborne data sets and supplementary ground data (see www.nafe.unimelb.edu.au; www.moisturemap.monash.edu.aaces; www.smapex.monash.edu) have been used to assess the representativeness of soil moisture sites for each of the 9 km x 9 km focus areas (areas YA and YB), corresponding to two pixels of the SMAP products at 3 km for radar, 9 km for radar-radiometer and 36 km for radiometer pixels (Yee et al. 2016). These stations have also been used to validate AMSR2 soil moisture products based on the JAXA and LPRM algorithm of different versions, and SMOS soil moisture products (Yee et al., 2016), and provide a perfect source of data for the passive-passive downscaling work proposed here.

Chapter 3: Flux Tower Maintenance for JFY2018

Regular site maintenance carried out during 2018 included visits to the JAXA Tower on a 1-2 monthly basis by a dedicated Monash technician. During these visits the following was completed as part of regular site checks; cleaning of the rain gauge, radiation sensors and solar panels, insect control and regular data downloads.

During May of 2018, two technicians attended site to complete a calibration of the Open Path CO₂/H₂O Gas Analyzer (LI-7500A). This included removing the sensor from the tower to undertake the calibration in controlled conditions (motel accommodation). The internal chemicals were replaced with cartridges purchased from LICOR and the unit was left to run (scrub CO₂) for 24 hours as per recommended in the manual. The calibration was undertaken the next day, with the sensor being returned to the tower within 48hours of removal.

Before calibration commenced, a visual inspection of the tower, guys and anchors was undertaken. However, technical staff have since advised the need for a formal inspection to be completed by a dedicated contractor. This is recommended to be done on an annual basis as per OzFlux guidelines. There is no record of this ever being done since installation. Enquiries have been made with a local contractor to undertake this inspection in the new fiscal year (JFY2019).



Figure 3: Calibration of the Open Path CO₂/H₂O Gas Analyzer (LI-7500A).



Figure 4: Monash technician climbing the tower to remove sensor for calibration.

It has been identified that the following sensors are giving erroneous data;

- TRIME-PICO32, 10 cm soil moisture sensor and temperature sensor
- Campbell Met One 034B Windset, 2 metre and 8 metre wind speed sensors

Following inspection of the ground sensors, it has been identified that there is no obvious physical damage and there is no problem with the wiring. Therefore, the sensors themselves must be faulty and complete replacement is needed.

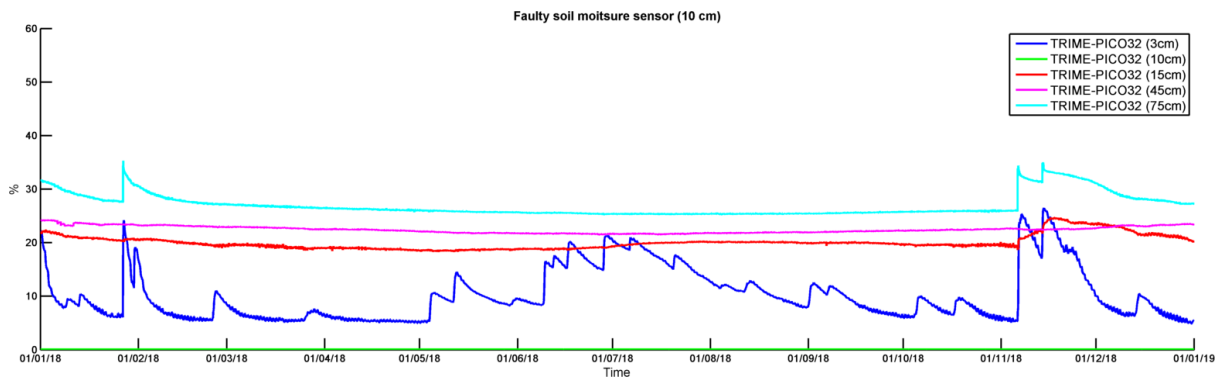


Figure 5: TRIME-PICO32, 10 cm soil moisture sensor (green) broken since Nov 2016.

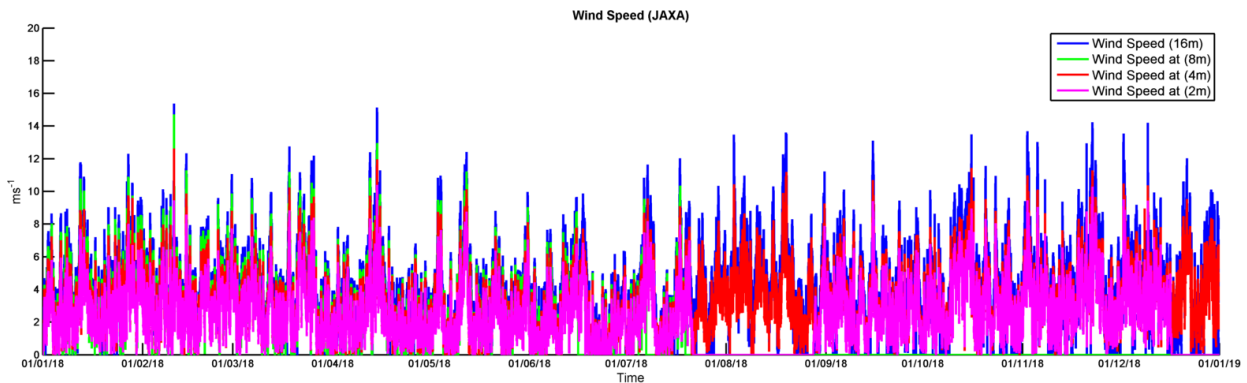


Figure 6: Campbell Met One 034B Windset; 8m (green) broken since late July 2018; 2m (pink) broken from July to August 2018 and from mid-December 2018 till present.

The two Campbell Met One 034B Windset sensors are unable to be inspected until a thorough tower inspection is completed (as stated above), which is scheduled for the next fiscal year (JFY2019). Once that is completed, we can advise whether a replacement for this is needed.

Due to a miscommunication, the HMP155 temperature and humidity sensor which was sent by JAXA was installed to the ASSH_T weather station instead of the tower. This is scheduled to be removed and re-installed on the tower at a height of 16m (where the old one was previously located) again, once the tower inspection is complete.



Figure 7: Mislocated Humidity and Temperature Probe (HMP 155) inside the Vaisala Weather Transmitter (WXT530), to be re-installed on to the tower at 16m height.

Chapter 4: Data Sets

4.1 Flux tower data updates for JFY2018

Half-hourly measurements from the JAXA flux tower are uploaded from the JAXA station to a Monash server on a weekly basis. The 10 Hz data are downloaded from the logger during monthly site visits. All raw data are downloadable from <http://www.oznet.org.au/mdbdata/mdbdata.html> (Figure 8).

OzNet Network Data Archive

PLEASE NOTE:

- The data provider accepts no responsibility for checking the accuracy of data accessed through this site and therefore makes no representation concerning its completeness, accuracy or its suitability for any particular purpose.
- This data set should be acknowledged by including the following reference:
Smith, A. B., Walker, J. P., Western, A. W., Young, B. L., Elwell, K. M., Pipunic, R. C., Grayson, R. B., Strawdena, L., Chew, F. H. S. and Richter, H. The Murrumbidgee Soil Moisture Monitoring Network Data Set. *Water Resources Research*, vol. 48, W07Z01, 6pp., 2012. doi:10.1029/2012WR011976
- Date and time of the data through this site are in AEST without daylight saving (JTC+10).
- Data is made publicly available through this website at the end of each season. A 12 months embargo period is applied. Please [contact us](#) if you would like more recent data, providing a description of the scope of your request.

[Important Documentation](#)
[JAXA variables description](#)

Individual sites and recording periods can be downloaded in Excel format from the links below. Data from soil moisture stations are available in seasons (su: Summer, au: Autumn, wi: Winter, sp: Spring). JAXA data is available on a half-yearly basis (01: Jan to Jun, 07: July to Dec).

Site: JAXA Station: Show: 10 Search:

Site	Station	Year	Period	Link
JAXA	WEATHER, RADIATION AND SOIL	2018	01	Download
JAXA	WEATHER, RADIATION AND SOIL	2018	07	Download
JAXA	WEATHER, RADIATION AND SOIL	2015	01	Download
JAXA	WEATHER, RADIATION AND SOIL	2014	07	Download
JAXA	WEATHER, RADIATION AND SOIL	2014	01	Download
JAXA	WEATHER, RADIATION AND SOIL	2017	07	Download
JAXA	WEATHER, RADIATION AND SOIL	2017	01	Download
JAXA	WEATHER, RADIATION AND SOIL	2019	01	Download
JAXA	WEATHER, RADIATION AND SOIL	2013	01	Download
JAXA	WEATHER, RADIATION AND SOIL	2016	01	Download

Showing 1 to 10 of 65 records Pages: [Previous](#) [1](#) [2](#) [3](#) ... [7](#) [Next](#)

Figure 8: JAXA data download interface on <http://www.oznet.org.au/mdbdata/mdbdata.html>.

Based on the recent proposal, simple quality checks will be applied to these data to remove data which are out of range and will be archived every 3 months. Figures below show some of the key data collected in 2018 from the JAXA tower.

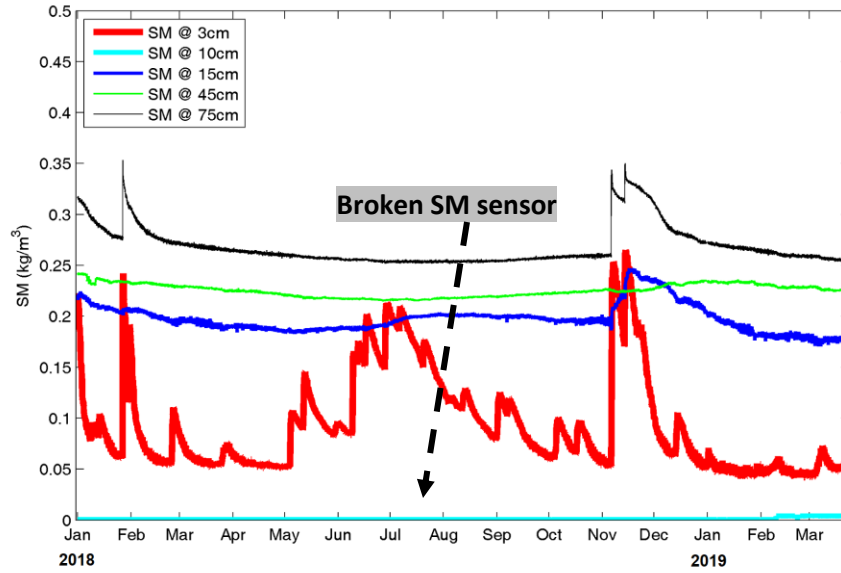


Figure 9: Soil moisture data at 3cm, 10cm, 15cm, 45cm and 75cm from the tower.

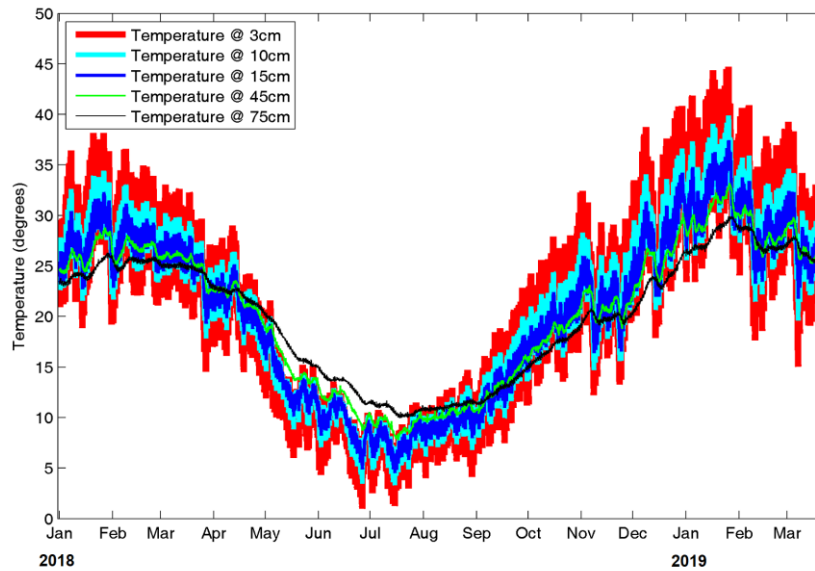


Figure 10: Soil temperature data at 3cm, 10cm, 15cm, 45cm and 75cm from the tower.

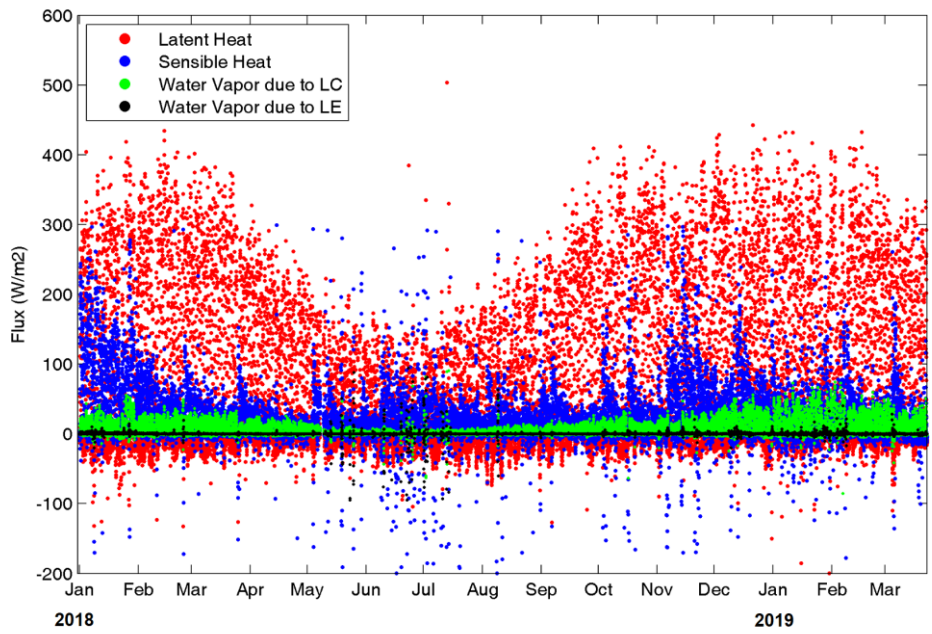


Figure 11: Latent/sensible heat and water vapor due to latent/sensible heat from the tower.

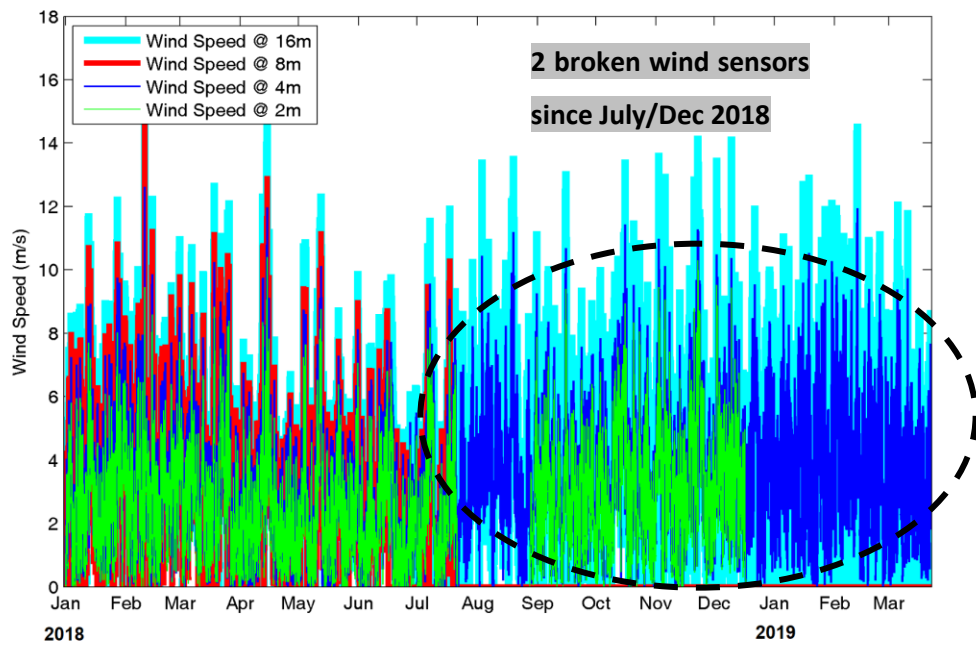


Figure 12: Wind speed at 2m, 4m, 8m and 16m measured from the tower.

Real-time figures from the flux tower is also produced and available at <http://www.science.uwa.edu.au/centres/land/yanco>. The website is maintained by Prof. Jason Beringer's team in Faculty of Science, the University of Western Australia (jason.beringer@uwa.edu.au).

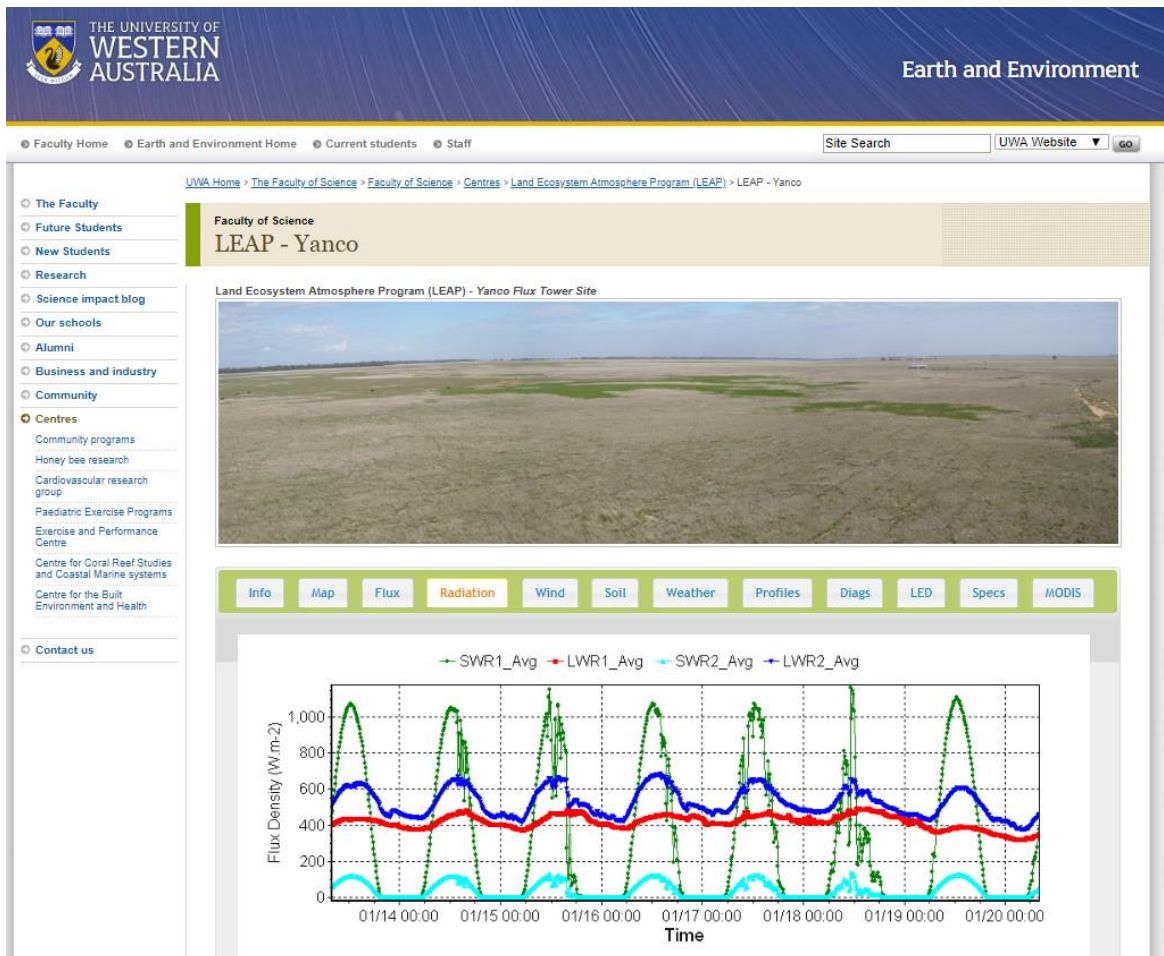


Figure 13: Real-time tower data interface on <http://www.science.uwa.edu.au/centres/land/yanco>.

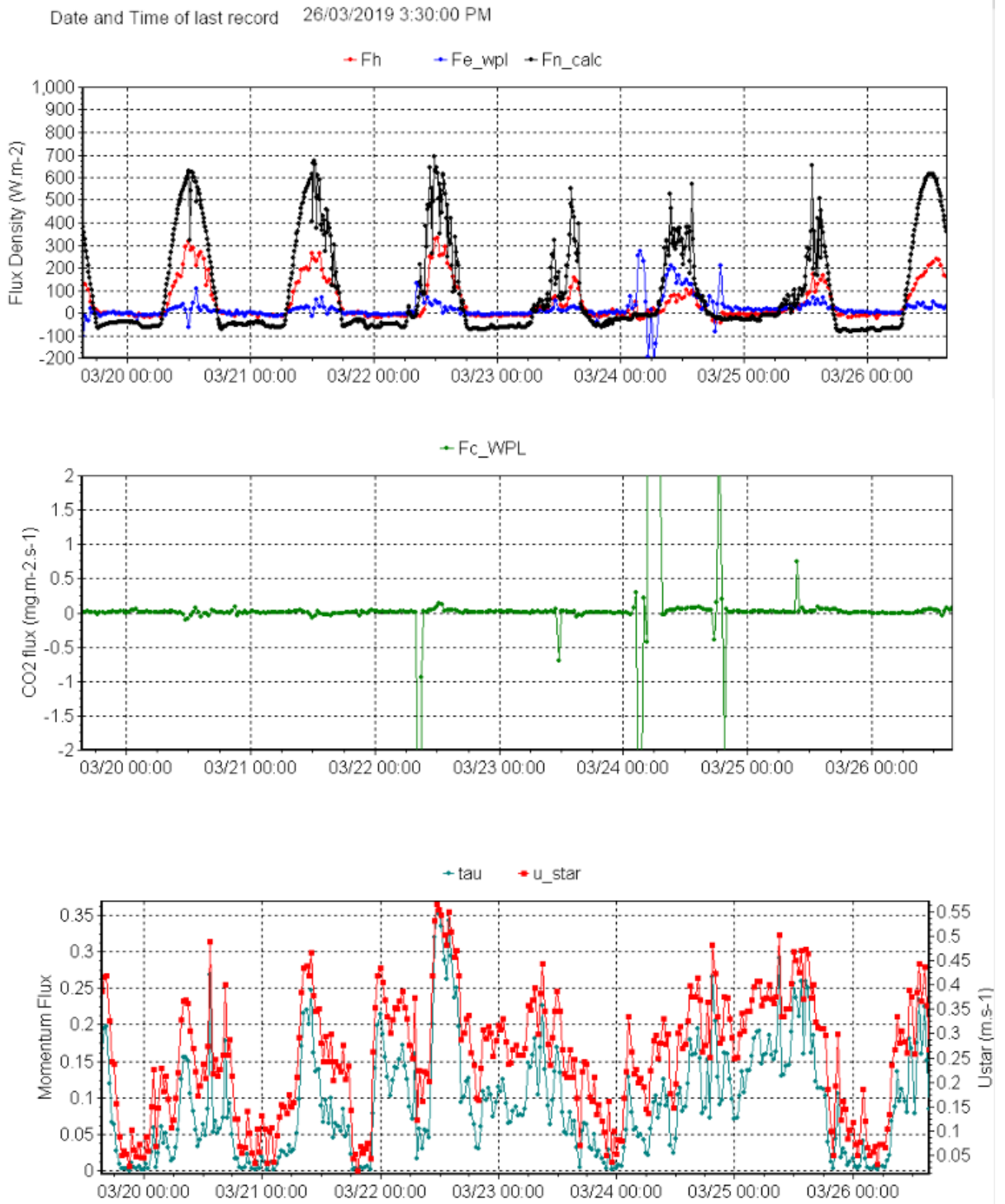


Figure 14: Examples of real-time figures for flux data available on the above website.

4.2 OzNet monitoring network data

Soil moisture and soil temperature over 20-min interval of measurements from the OzNet monitoring stations are collected from each station. All raw data have been archived and downloadable at <http://www.oznet.org.au>.

Data were separated and named according to the southern hemispheric seasons, i.e. spring (September – November), summer (December – February), autumn (March – May) and winter (June – August). Simple quality checks have been applied to these data whereby out of range values have been removed. An example of the data collected from station YA5 from autumn to summer for 2018 are display in the following page.

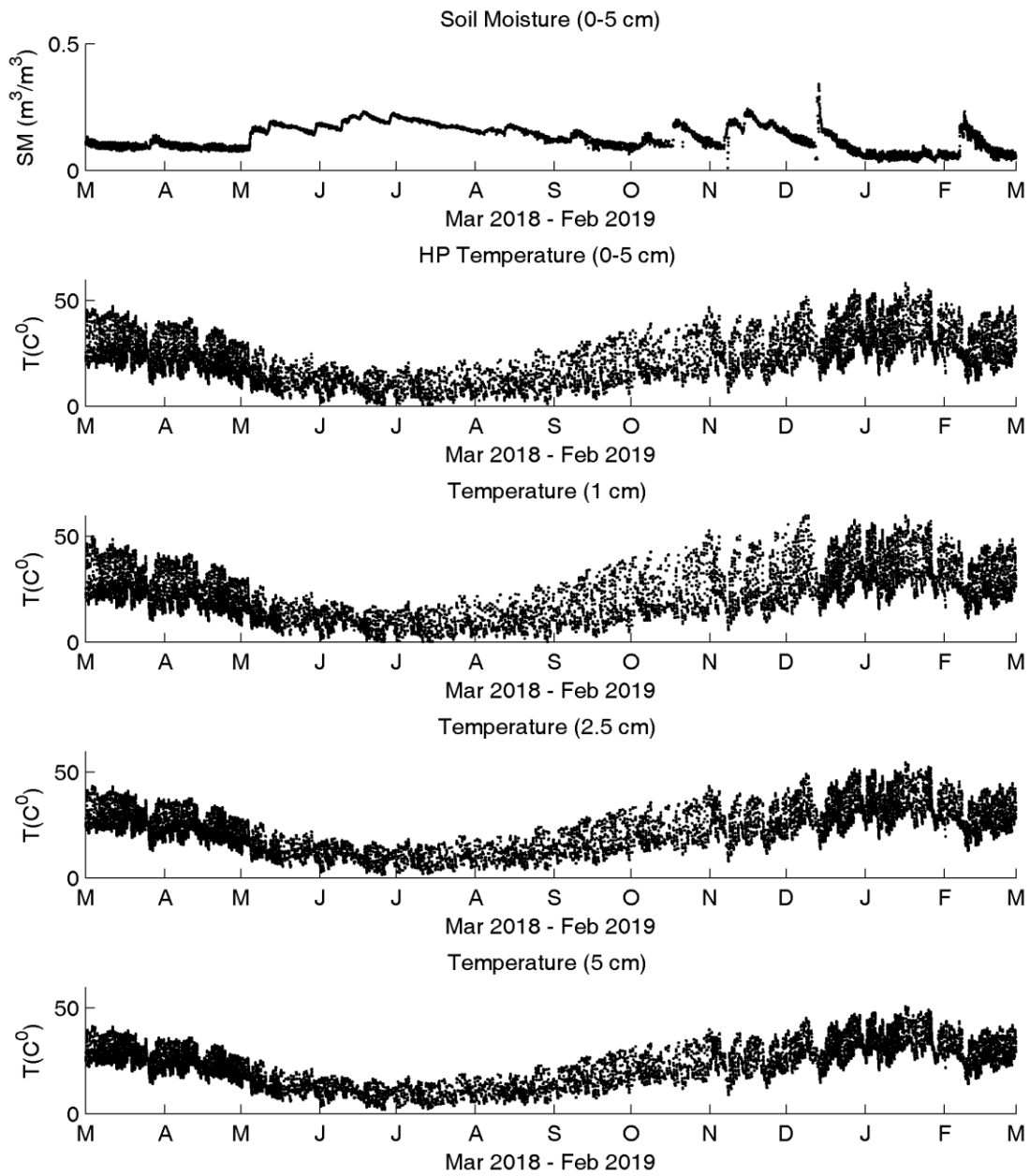


Figure 15: Example of soil moisture and temperature collected from YA5 from March 2018 to February 2019.

4.3 Airborne brightness temperature data

The fourth and fifth Soil Moisture Active Passive Experiments (SMAPEX-4 & -5) were conducted in the austral autumn, from 1st May to 22nd May 2015, and in the austral spring, from 7th September to 27th September 2015, respectively at the Yanco area. The main objective was to collect airborne active and passive microwave brightness temperatures, ground observations of soil moisture, and ancillary data needed for soil moisture retrievals in coincidence with SMAP coverage, providing microwave observation and soil moisture references for SMAP in-orbit validation. The SMAPEX-5 study area and flight areas are shown in Figure 16.

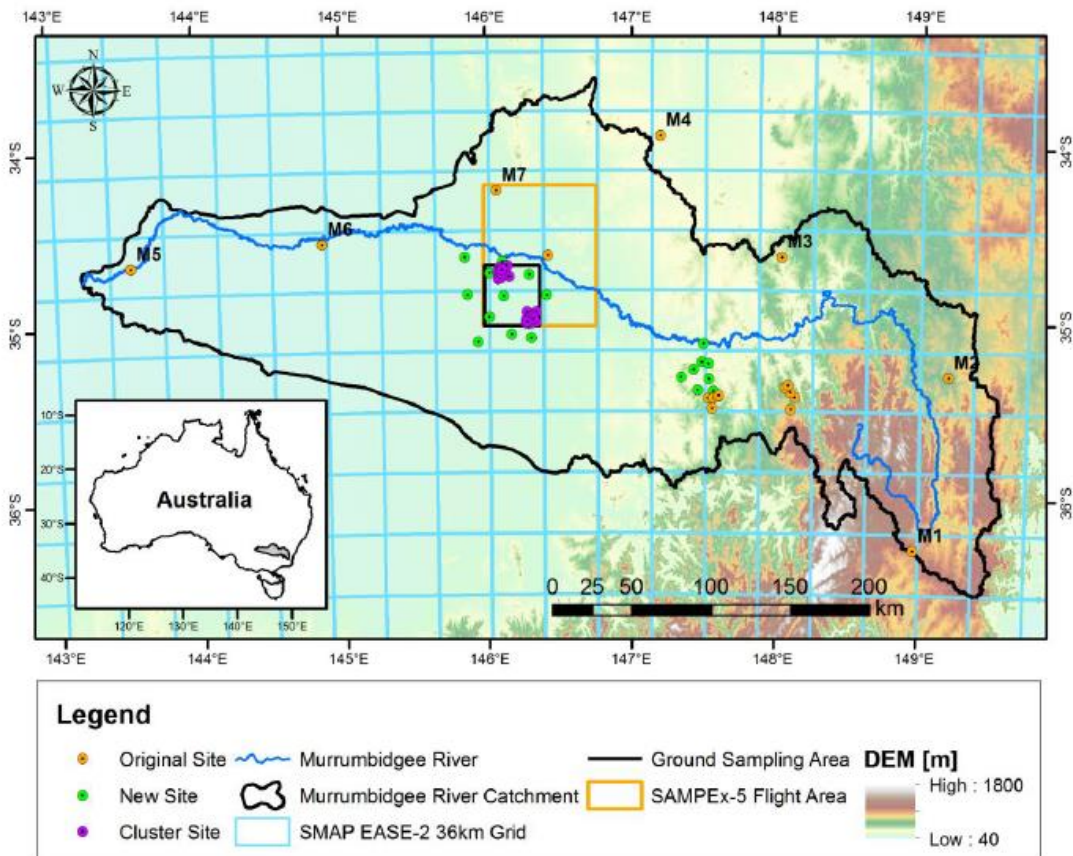


Figure 16: Study area and airborne monitoring are during SMAPEX-5

Soil moisture has been retrieved from both campaigns for the Yanco site from airborne passive microwave observations at 1 km resolution. The passive airborne sensor is called The Polarimetric L-band Multibeam Radiometer (PLMR), which measures brightness temperature at both V and H polarisations using a single receiver with polarisation switch at incidence angles $\pm 7^\circ$, $\pm 21.5^\circ$ and $\pm 38.5^\circ$ in either across-track or along-track configuration. The airborne brightness temperature measured at vertical polarization at 1-km resolution is shown in Figure 17 (SMAPEX-4) and Figure 18 (SMAPEX-5).

Ground sampling was undertaken concurrently with the flights and mainly included intensive spatial soil moisture sampling in six focus areas, as well as the regional soil moisture sampling in SMAPEX study area.

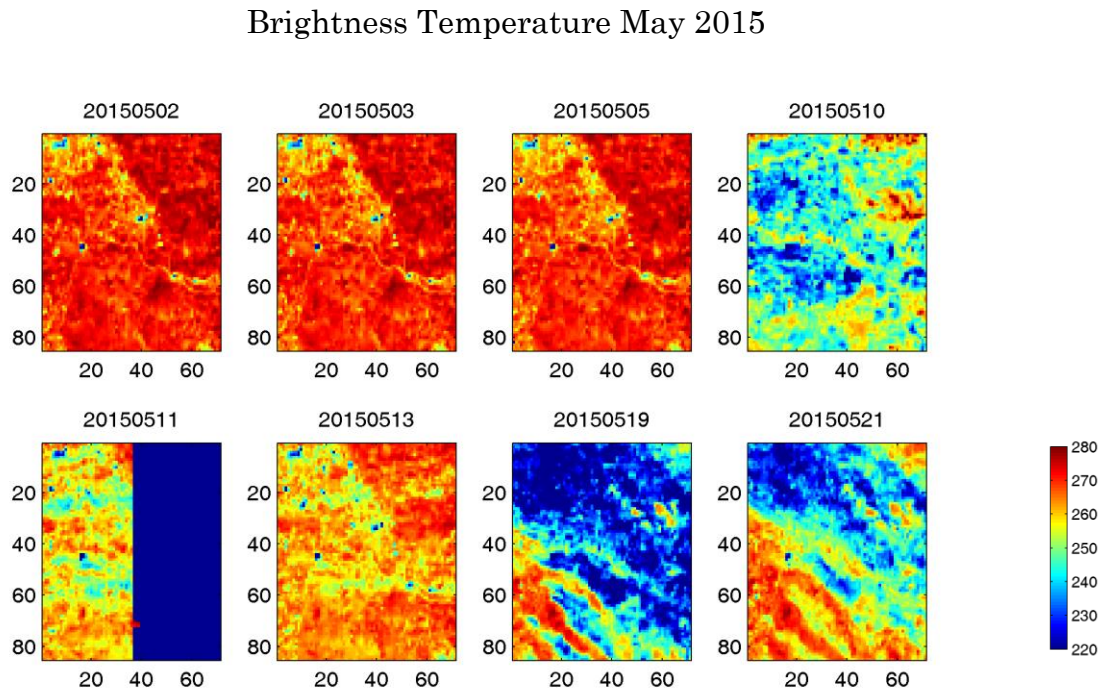


Figure 17: Airborne brightness temperature at V-polarization from SMAPEX-4 at Yanco area. Title of each subplot indicates flight date with the format of YYYYMMDD.

Brightness Temperature September 2015

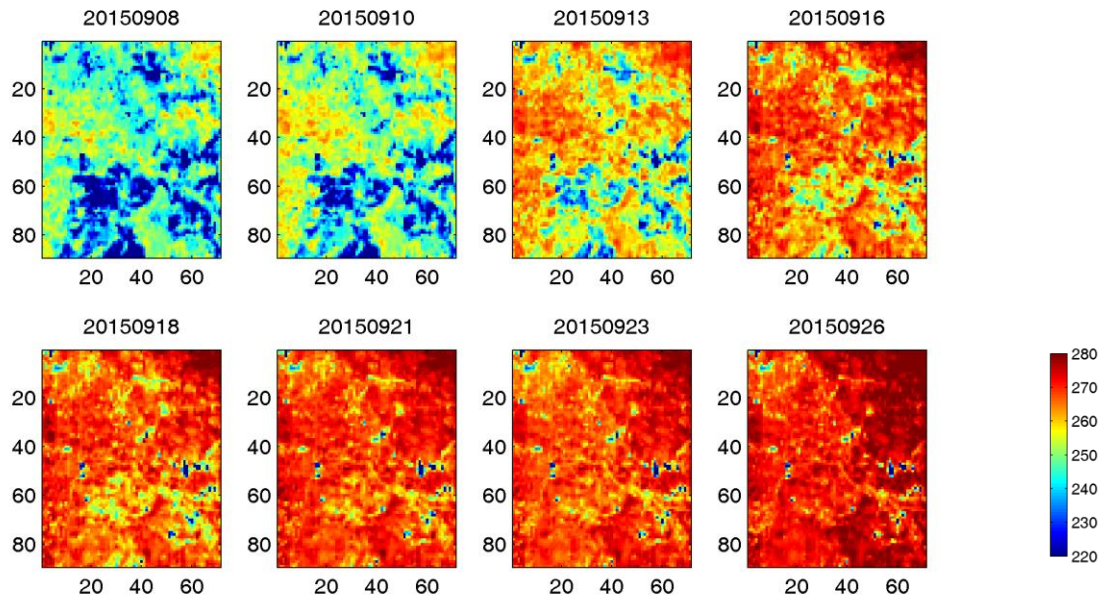


Figure 18: Airborne brightness temperature at V-polarization from SMAPEX-5 at Yanco area. Title of each subplot indicates flight date with the format of YYYYMMDD.

4.4 AMSR2 Level 3 soil moisture product

The AMSR2 L3 soil moisture product was downloaded from the GCOM-W1 Data providing Service (gcom-w1.jaxa.jp/index.html). To cover the whole period in which AMSR2 data is available, the analysis covered a time series from July 2012 to December 2018. Both the high resolution 10-km product and the low resolution 25-km product were considered in the analysis. The identifier for the two types of products are GW1AM2_YYYYMMDD_01D_EQMD_L3SGSMCHF3300300 and GW1AM2_20120706_01D_EQMD_L3SGSMCLF3300300, respectively.

The AMSR2 pixel in which JAXA tower (-34.99S, 146.29E) is located was extracted. The pixel location of the L3 SM data scene is Row 1250, Column 1463 for the 10-km product, and Row 500, Column 586 for the 25-km product. The pixel boundaries with respect to the flux tower location is shown in Figure 19.

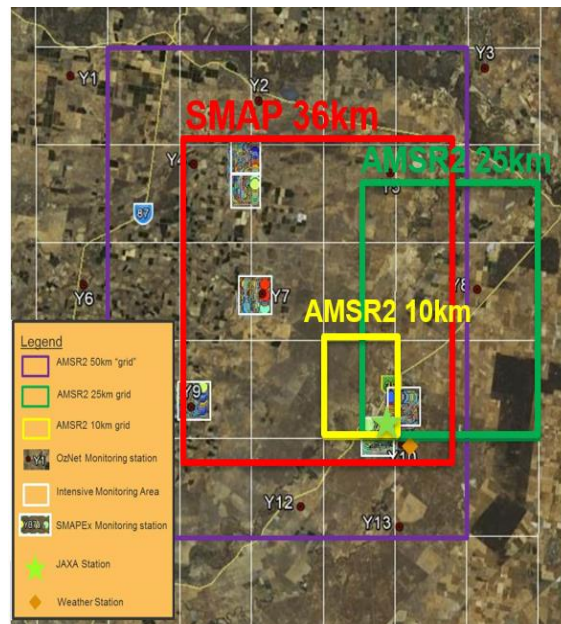


Figure 19: Location of the 10-km and 25-km AMSR2 L3 SMC pixel, SMAP 36-km pixel with respect to the flux tower location.

The time series of the AMSR2 L3 SMC 10-km and 25-km products are shown in Figure 20. Comparing with 2015-2017, 2017-2019 experienced a dryer condition throughout the period. The wet season (May to August) in 2017-2019 is clearly shorter and has less extreme in rainfall events. It can also be seen the high-resolution soil moisture almost coincide with the low-resolution data, especially during the dry season. During the wet season, however, the low-resolution soil

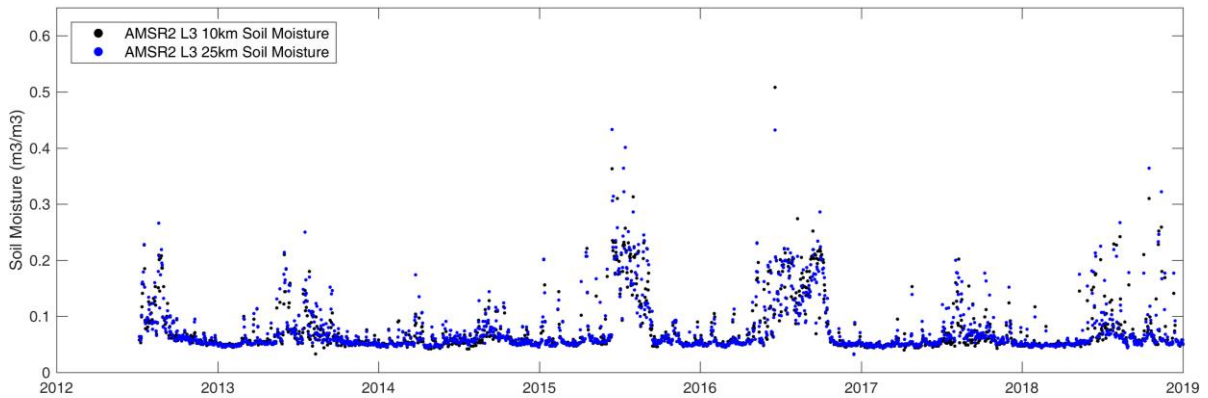


Figure 20: Time series of the AMSR2 L3 10-km and 25-km soil moisture in the Yanco site.

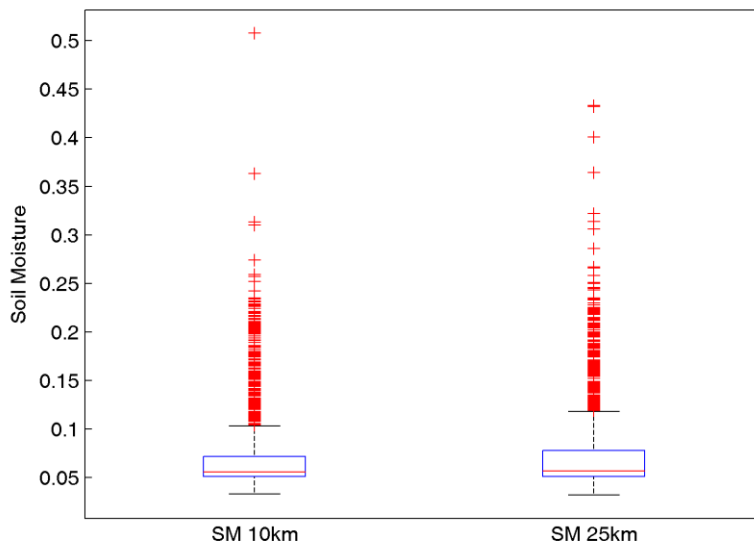


Figure 21: Box plot of the AMSR2 L3 10-km and 25-km soil moisture in the Yanco site.

moisture has a relatively larger dynamic range. This could be due the reason that 25-km pixel contains a larger area and thus include mixed land cover types such as pasture, crops and forest, which the 10-km pixel is almost pasture.

Figure 21 which show the box plots of the AMSR2 L3 low- and high- resolution soil moisture. It is seen that most of data fall in the range of $0.03 \text{ m}^3/\text{m}^3$ to $0.12 \text{ m}^3/\text{m}^3$ and the average is only slightly above $0.05 \text{ m}^3/\text{m}^3$. Very few data exceed $0.2 \text{ m}^3/\text{m}^3$ which mostly happened in the winter season of 2015 and 2016, with the highest reaching $0.5 \text{ m}^3/\text{m}^3$.

Chapter 5: Validation of AMSR-2 Level 3 soil moisture products

5.1 Time series

The AMSR2 L3 low- and high-resolution soil moisture products are validated against 1) the in-situ soil moisture measurements from the JAXA flux tower, 2) in-situ soil moisture measurements from OzNet stations and 3) SMAP observations.

On the flux tower, soil moisture sensor was installed at 3 cm depth below ground. A time series plot of the comparison from January 2017 to January 2019 is shown in Figure 22. It is seen that the AMSR2 products (black and blue) are underestimating the tower soil moisture (red) in general. The correlation is relatively higher during the dry period of year 2017-2018. Unlike year 2017, the offset between tower measurements and AMSR2 soil moisture product during 2018 is significantly smaller in wet seasons (May-August).

In winter of 2018, AMSR2 observation successfully managed to capture the part of the soil moisture increase and the variation pattern. However, from August to November of 2018, while in-situ measurements were gradually drying down, a couple of satellite observations exceeds the ground 'truth' by 0.1-0.2 m³/m³.

There are two main reasons which might lead to the discrepancies:

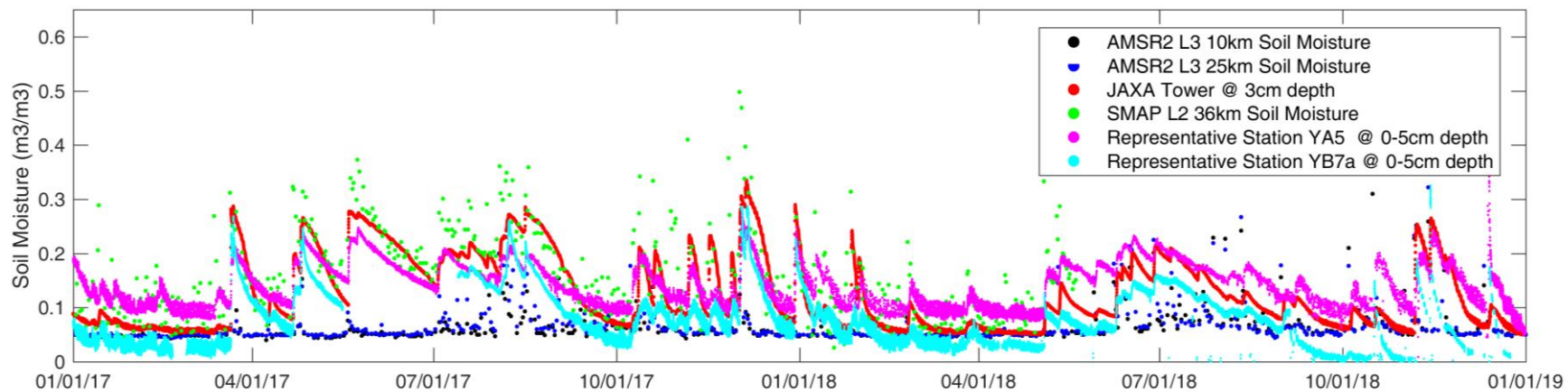


Figure 22: Time series plot of AMSR2 L3 10- and 25-km soil moisture product against JAXA flux tower soil moisture measured at 3-cm depth.

- i) Flux tower measurement is only a ‘point’ measurement which only reflect the situation at or immediately around the station, while the satellite product corresponds to a larger area;
- ii) The soil moisture retrieval algorithm of the AMSR2 L3 product is based on the brightness temperature (TB) observation at 10 GHz (V, H) and 36 GHz (V). The microwave signal at such frequencies was emitted from the very top of the ground surface (less than 1 cm depth) and was relatively more sensitive to the overlaying vegetation compared with lower frequencies, while the tower moisture sensor was measuring the soil moisture at a deeper layer of 3 cm.

The comparison of the AMSR2 products against the OzNet stations shows similar results as above. Two stations within the network, YA5 (pink) and YB7a (sky blue), which were previously demonstrated to be the most representative of the entire Yanco area (Yee et al., 2016), were chosen for the validation. From the time series of the satellite and station soil moisture plotted in Figure 22, it is seen that the AMSR2 product is again underestimating the soil moisture ‘truth’ measured by the in-situ sensor. Except that the OzNet station measurements represent an average value of the surface soil profile from 0 to 5 cm, the two main reasons of the discrepancy summarized above apply here as well.

The AMSR2 L3 products are also compared against the Soil Moisture Active Passive (SMAP) L3 product which was retrieved from L-band (1.4 GHz) brightness temperature observations. SMAP has a larger footprint of 36 km compared with AMSR2 (Figure 19). Time series of the SMAP product is also plotted in Figure 22. It is seen while SMAP product is significantly higher than AMSR2, especially during the wet season, it has a better correlation with the in-situ measurement from the

JAXA tower. Since it has also been widely demonstrated in the past that low frequency (such as L-band) has higher sensitivity to the moisture content variation and more capable to retrieve accurate surface soil moisture, it is suggested that the SMAP product should be closer to the ‘truth’, and further improvement of the AMSR2 retrieval algorithm will be needed.

As also mentioned in the annual report of JFY 2017, one possible way for improving the AMSR2 soil moisture product is through applying a simple regression of itself against in-situ measurement based on the historical data profile. This regression could be set to apply to the original product once soil moisture exceeds certain level, e.g. $0.1 \text{ m}^3/\text{m}^3$, beyond which the product/in-situ discrepancy starts to become more pronounced. Research of this methodology is being investigated.

5.2 Scatter plots

The AMSR2 L3 soil moisture product at 10-km resolution are also plotted in Figure 23 as scatters against soil moisture observations from tower, SMAP, station YA5 and YB7a, respectively. It is seen that the AMSR2 L3 product has an underestimation when compared with all four different references, with a negative bias ranging from $0.02 \text{ m}^3/\text{m}^3$ to $0.09 \text{ m}^3/\text{m}^3$.

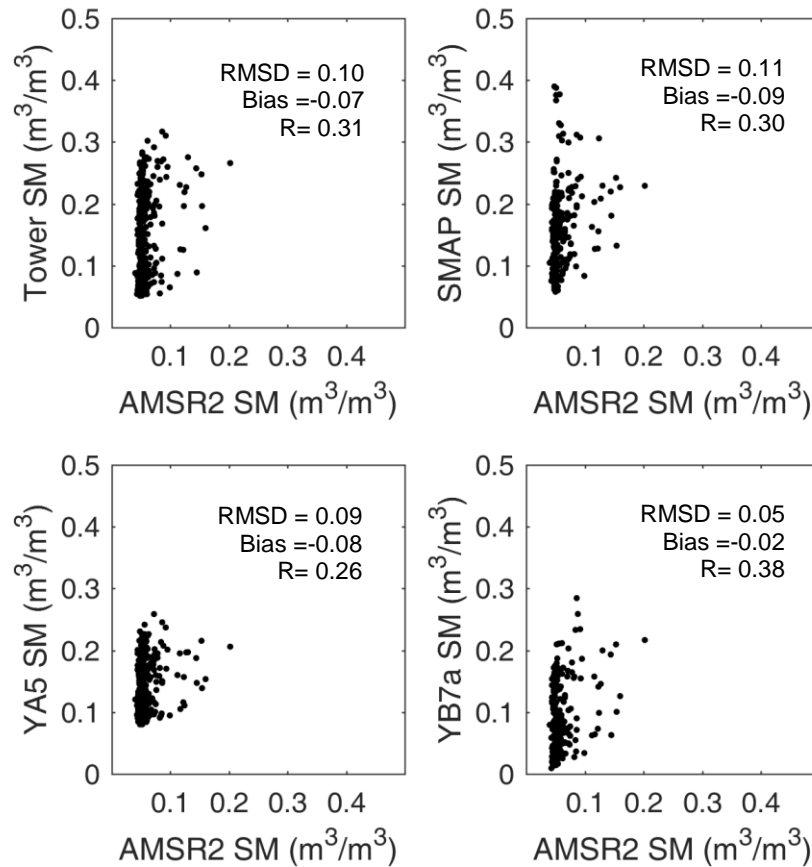


Figure 23: Scatter plots of AMSR2 SM (10-km) against soil moisture from the tower, SMAP observations, YA5 station and YB7a station.

In order to assess the accuracy of the tower soil moisture measurements, tower soil moisture is also plotted against AMSR2 product, SMAP product and the two OzNet station measurement, respectively (Figure 24). Statistics are also calculated to quantify the accuracy. Results show the tower observations match better with the SMAP product with an accuracy of 0.04 m³/m³ and a very small 0.01 m³/m³ bias. Tower soil moisture also has a relatively good agreement with the two

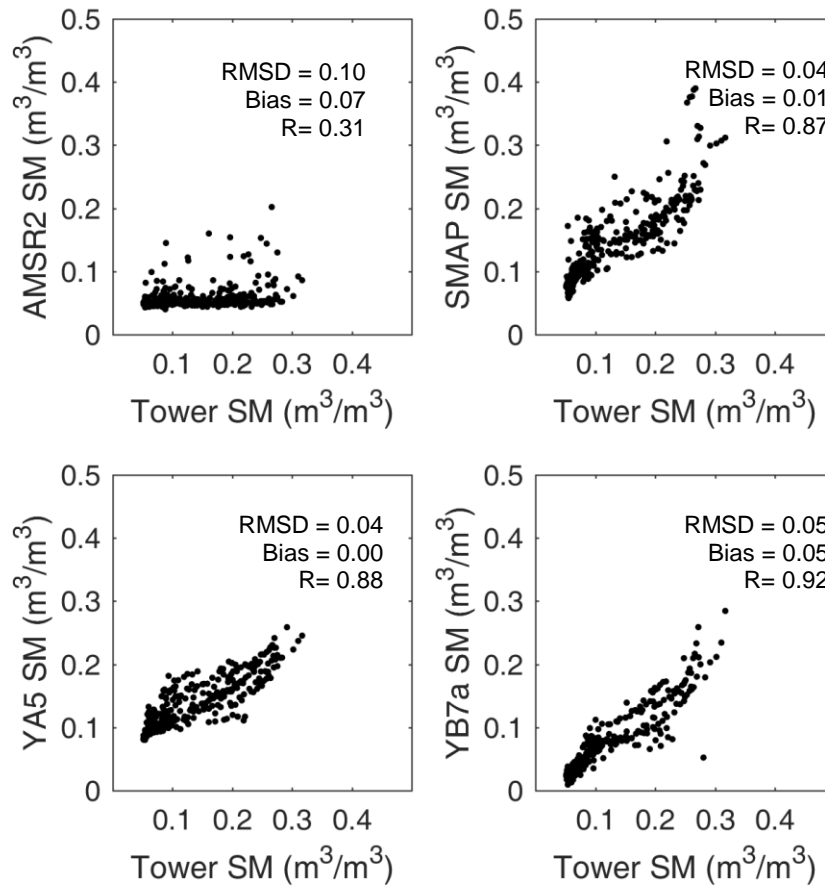


Figure 24: Scatter plots of tower soil moisture against AMSR2 SM (10-km), SMAP SM (36-km), YA5 and YB7a station soil moisture.

representative OzNet stations, with accuracy smaller than $0.05 m^3/m^3$ and superior correlation of higher than 0.88. This means that tower measurements are closer to the soil moisture ‘truth’ and is reliable as a source of validation tool.

Figure 25 shows the AMSR2 validation scatter plots in 2017-2018 compared with in 2015-2016. It shows that recent data sets are more condensed, and data dynamic range is smaller in terms of both satellite and in-situ observations compared with

two years earlier. This again means the Yanco site has experienced a dryer condition during 2017-2018.

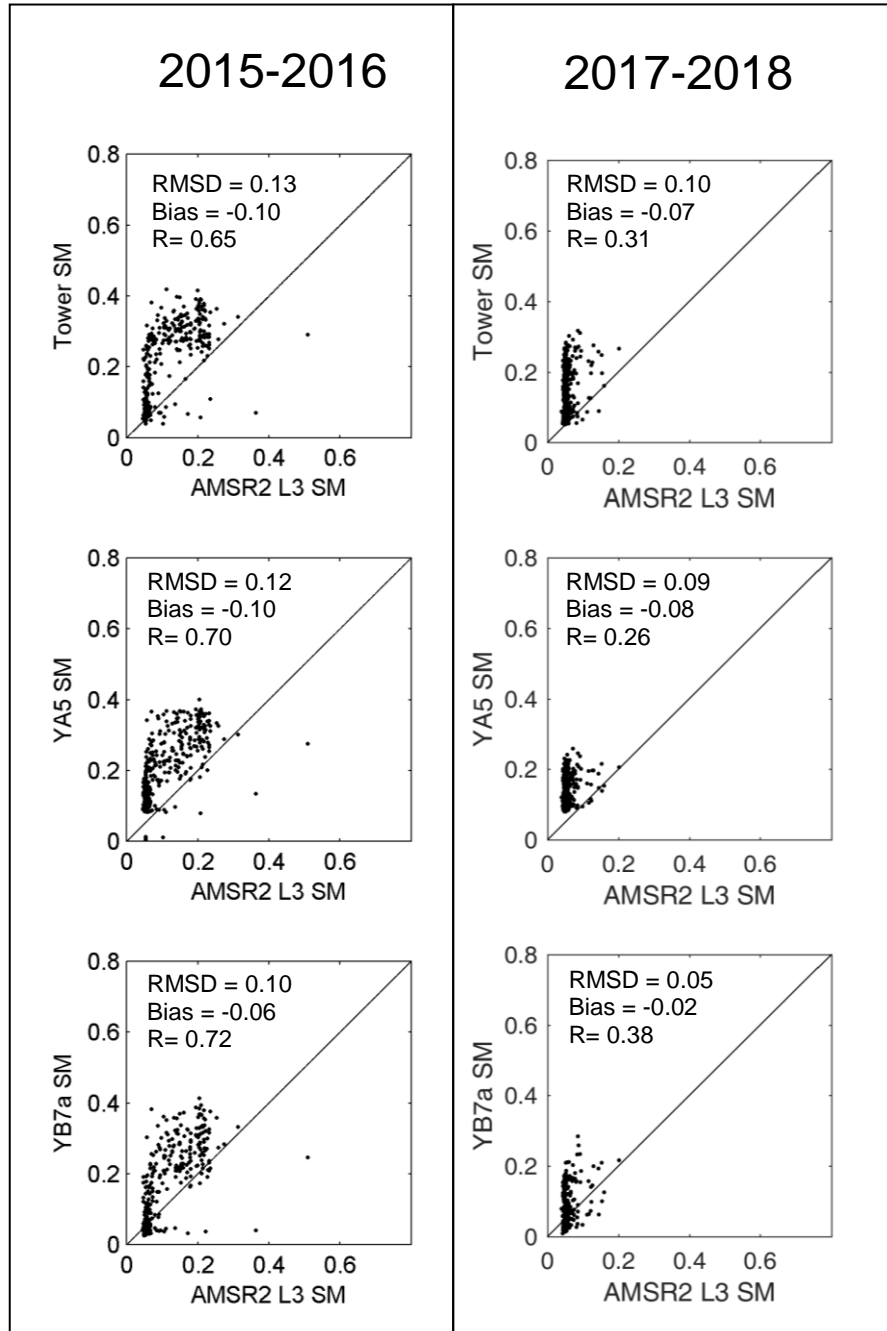


Figure 25: Comparison of AMSR2 L3 SM validation in 2017-2018 against 2015-2016.

Chapter 6: Downscaling of low-resolution C-band Brightness Temperature from AMSR2

6.1 The SFIM downscaling methodology

Soil moisture products at spatial resolutions finer than the AMSR2 footprint are important for many hydro-meteorologic applications. Consequently, we propose to use higher resolution Ka-band brightness temperature (TB) data from AMSR2 to downscale its low-resolution C-band TB data using passive-passive downscaling techniques. The smoothing filter-based modulation (SFIM) technique (Liu, 2000) has been chosen to be the primary option for downscaling. The advantage of this technique is that all observations are made from the same platform, thereby avoiding issues regarding differences in observation times. It was suggested by Santi (2010) for soil moisture downscaling and has also been applied by Jeu et al., (2014), Parinussa et al., (2014) and Gevaert et al., (2015). Furthermore, we propose to validate the downscaled results against in-situ station data, as well as intensive soil moisture sampling data and airborne soil moisture product from the SMAPEX campaign.

In this downscaling technique, the Ka-band TB observations are aggregated to the resolution of the C-band using a low pass filter. Subsequently, the ratio between the high- and low-resolution Ka-band TB is used to modulate the low-resolution C-band TB of both polarizations by the following equation:

$$TB_{C-high} = TB_{Ka-high} / TB_{Ka-low} \times TB_{C-low} \quad \text{Eq. 1}$$

where the subscripts in Eq. 1 refer to the frequency bands and resolutions, respectively. This technique assumes that the variability within a C-band footprint is linked to the variability in the Ka-band.

Since the higher frequency of Ka-band signal is more sensitive to attenuation by vegetation and thus less sensitive to soil moisture than longer wavelengths such as

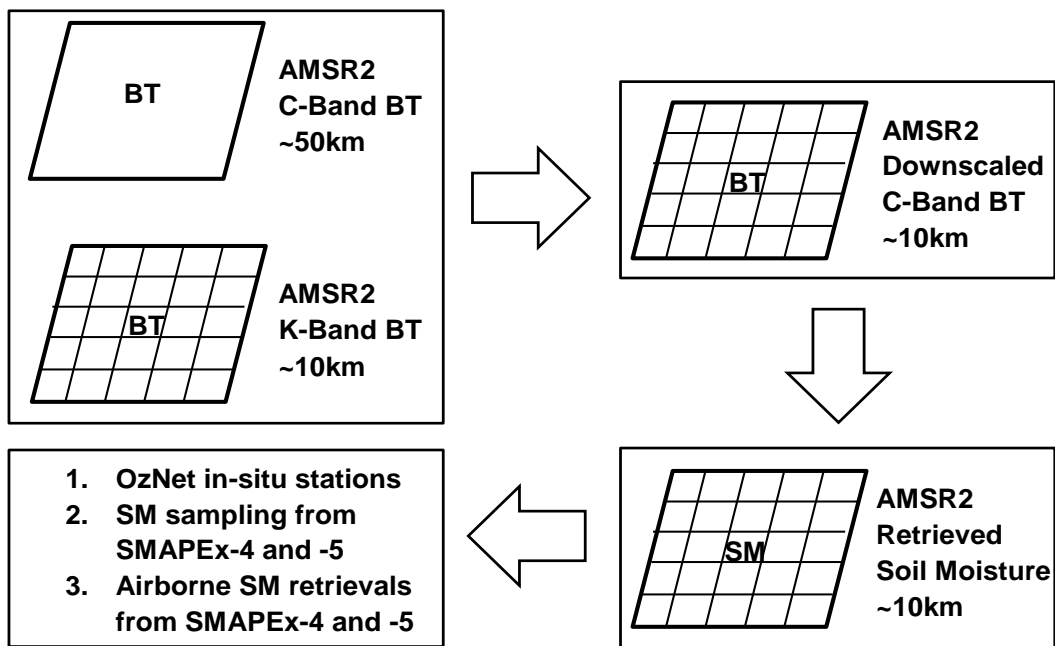


Figure 26: A schematic plan for AMSR2 soil moisture downscaling and validation procedures.

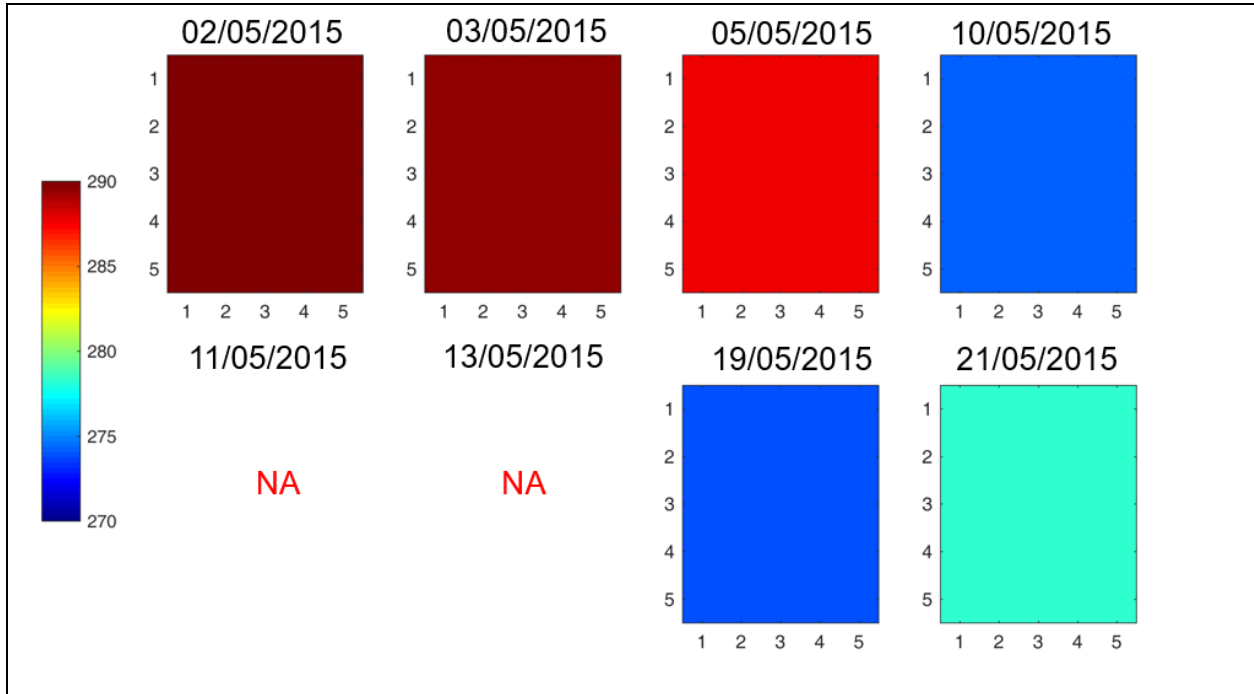
the C-band, the Ka-band TB, therefore, is not used in the later soil moisture retrievals. Even so, this enhanced sensitivity to vegetation could potentially impact the quality of sharpened soil moisture products over densely vegetated areas. More details about this technique can be found in Santi (2010), Jeu et al., (2014), Parinussa et al., (2014) and Gevaert et al., (2015). A schematic plot of the downscaling and validation processes is shown in Figure 26.

6.2 Input: AMSE-2 C-band and Ka-band TB products

The AMSR2 L1R brightness temperature product was downloaded from the GCOM-W1 ftp server. The product identifier is GW1AM2_YYYYMMDDHHMM_XXXD_2220220. The 6 GHz – V and – H (C-band) and 36 GHz – V and – H (Ka-band) TB data were extracted from the original product. The study period was initially focused on May 2015, for better comparison and validation with the SMAPEX field campaign. We chose the non-gridded original swath data because it is the actual values derived from AMSR2 observations and thus avoiding the averaging affect happened during the gridding process. Swath data is provided at a resolution of ~10km, which means there were significant over-sampling at low resolution (i.e. C-band) but are nearly independent at high resolution (Ka-band in this case).

Figure 27 and 28 shows the C-band (50-km) and Ka-band (10-km) brightness temperature map for the Yanco area, ascending and descending respectively, during the SMAPEX-4 campaign period. The high-resolution Ka-band data has a more detailed spatial pattern. Compared with the descending data (AM), the ascending data (PM) has more variance throughout the entire month. The brightness temperature (TB) is warmer at 1:30pm during the beginning of the month (2nd, 3rd of May) and became cooler later in the month (19th, 21st of May). However, at

TB – Ascending (1:30pm), C-band at 50-km, V-pol



TB – Ascending (1:30pm), Ka-band at 10-km, V-pol

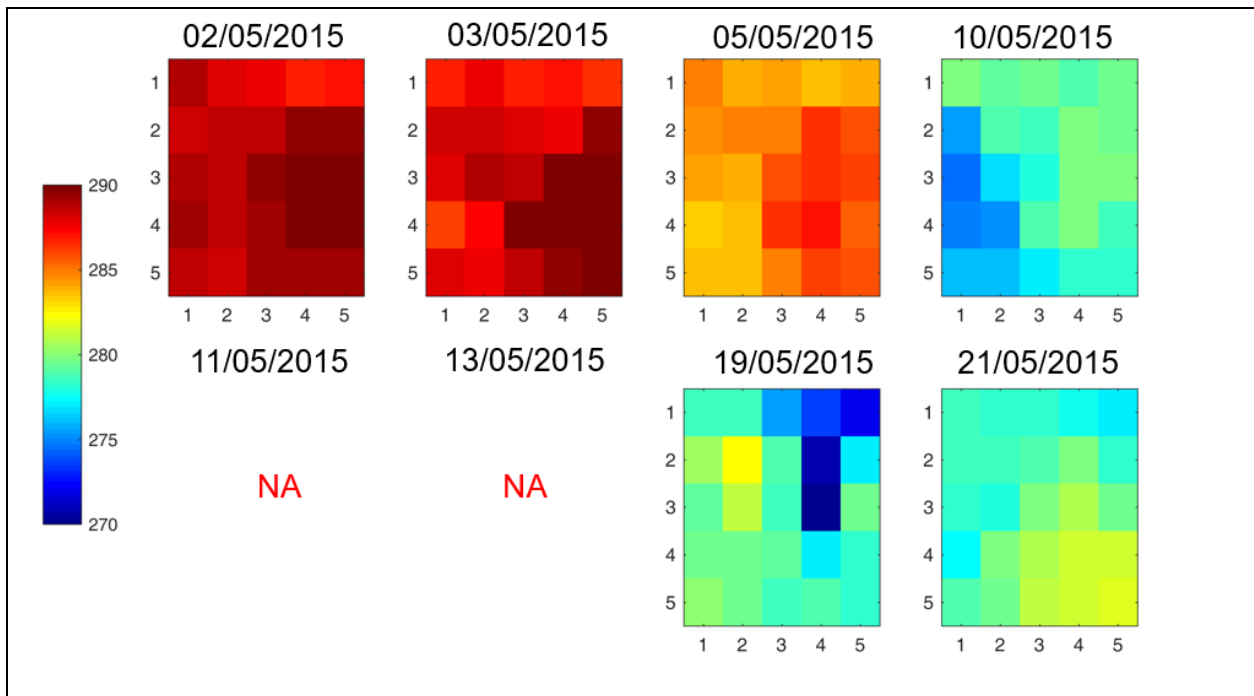
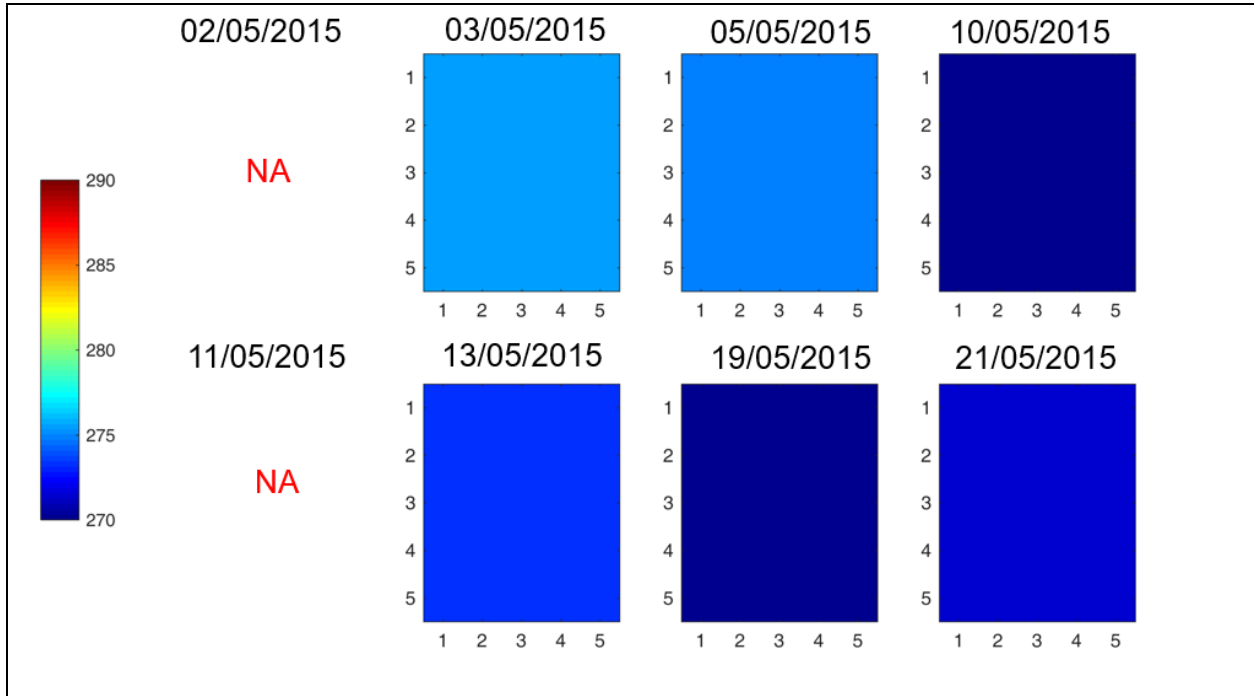


Figure 27: AMSR2 L1B map of C-band and Ka-band TB (Ascending) over SMAPEX-4.

TB – Descending (1:30am), C-band at 50-km, V-pol



TB – Descending (1:30am), Ka-band at 10-km, V-pol

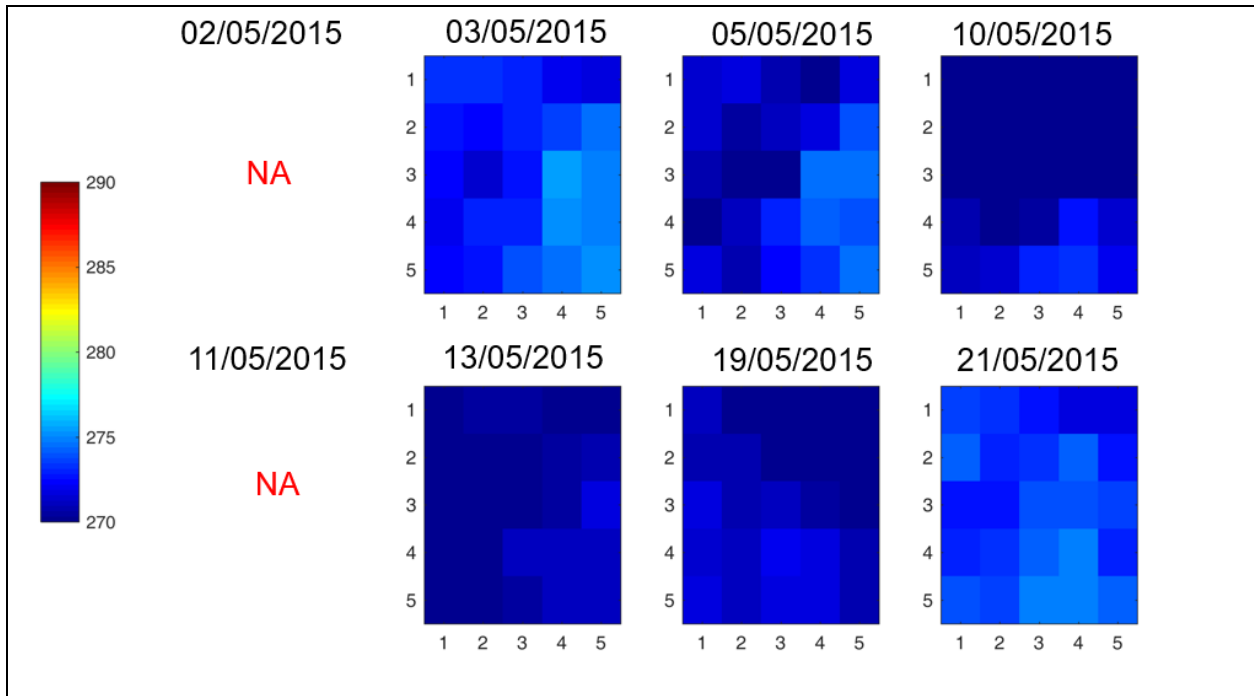


Figure 28: AMSR2 L1B map of C-band and Ka-band TB map (Descending) over SMAPEX-4.

1:30am, TB data is more consistent throughout the month. This is because TB is primarily determined by physical temperature. During midnight the physical temperature is more stable compared with in the afternoon.

From the Ka-band TB data, it is shown that spatially the southeast part of the Yanco area appears slightly warmer than the northwest. This could be due the spatial difference in soil type and vegetation land cover.

As there were no ascending overpasses on 11th and 13th of May, and no descending overpasses on 2nd and 11th of May, the special maps are not available. Therefore, downscaling is not applicable to those days.

6.3 Output: Downscaled C-band TB product

According to Equation 1, the Ka-band TB observations are aggregated to the resolution of the C-band, which is 50-km, using simple averaging. Subsequently, the ratio between the low-resolution C-band TB and the aggregated low-resolution Ka-band TB can be plotted, as shown in Figure 29.

A linear regression was fitted to the scatters to determine the relationship. In the case of Yanco site, the relationship of 50-km Ka-band TB against 50-km C-band TB is described as below:

$$TB_C = 1.118 TB_{Ka} - 52.88 \quad \text{Eq. 2}$$

The relationship gives a correlation of higher than 0.85 which is considered to be high enough to modulate the low-resolution C-band TB.

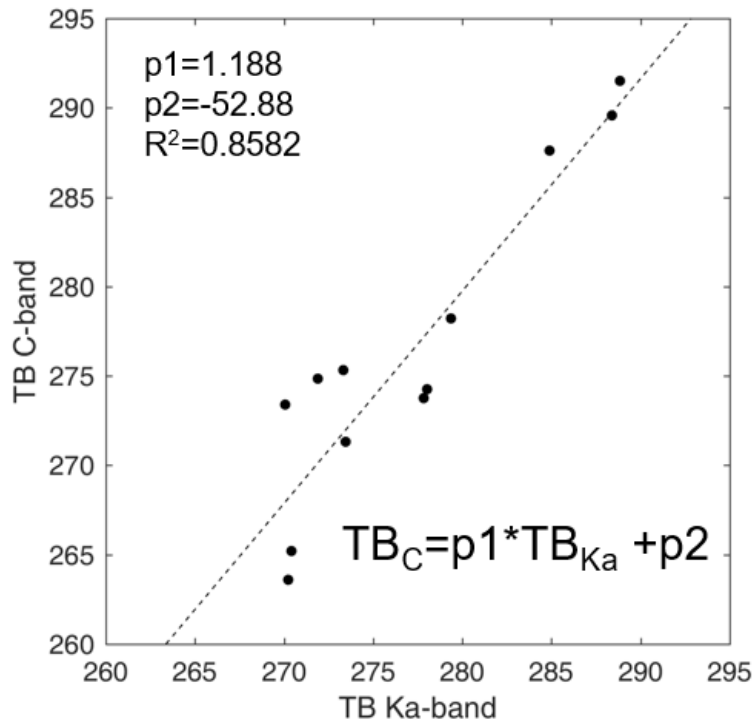


Figure 29: Linear regression between aggregated Ka-band and C-band brightness temperature at 50-km resolution.

The downscaled C-band TB maps at 10-km during the SMAPEX-4 period are shown in Figure 30. Also shown as a comparison are the L-band airborne TB measurements by the PLMR radiometer.

In order to validate the downscaled C-band TB, L-band airborne TB measurements at 1-km are aggregated to 10-km resolution and plotted as scatters against C-band TB. This is compared to the low-resolution SMAP L-band TB at 36-km against AMSR2 C-band L1B TB which was gridded to the same resolution, shown in Figure 31. The high-resolution C- to L-band relationship align very well with the low-resolution C- to L-band relationship.

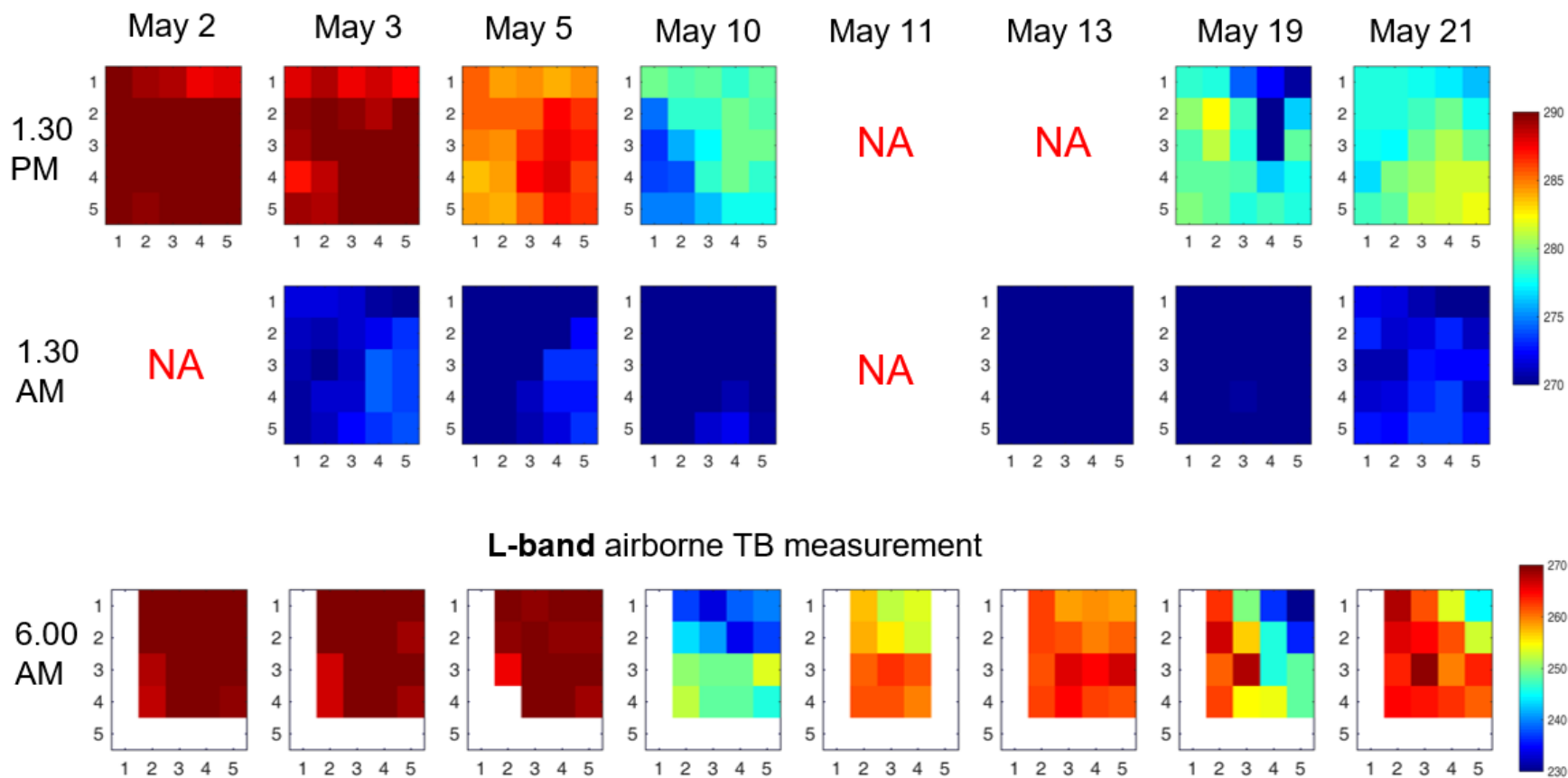


Figure 30: Downscaled C-band TB at 10-km resolution during SMAPEX-4 (PM and AM); Airborne L-band TB measurements by PLMR at the same days (AM).

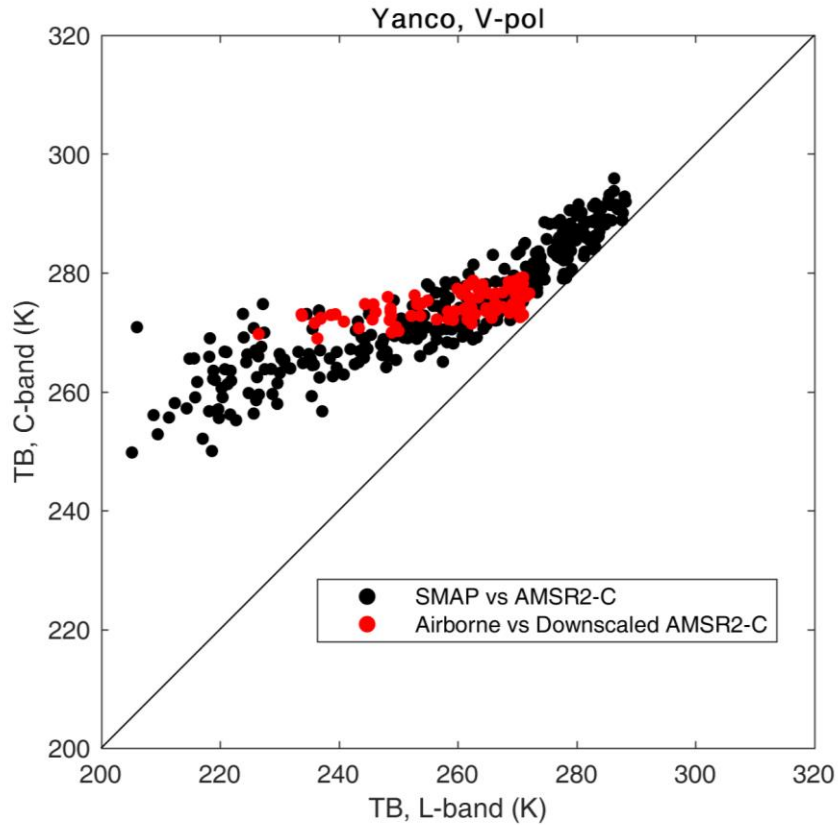


Figure 31: Correlation between C-band and L-band brightness temperature from satellite and airborne campaign measurements.

Currently, the research of soil moisture retrieval from the downscaled C-band brightness temperature is still underway.

Single Channel Algorithm was used for soil moisture retrieval of the downscaled brightness temperature. In this algorithm, soil moisture is retrieved using the tau-omega model. The model parameters are calibrated based on the soil moisture and surface temperature measurements from in-situ stations. Two most sensitive parameters: vegetation parameter b and roughness parameter h , will be calibrated simultaneously at both horizontal and vertical polarizations. The optical depth τ

is estimated from b and vegetation water content (VWC), which can be calculated from MODIS NDVI product. The calibration is performed while compromising between two criteria: 1) minimization of the Root Mean Squared Difference (RMSD) of simulated and observed TB, and 2) maintaining the dynamic range of the time series as close as to the satellite signals. The calibrated b and h are then applied for soil moisture retrieval using the downscaled AMSR2 C-band observations.

Chapter 7: Summary and Conclusion

This report presents the JFY 2018 research results for the project ‘Validation of global water and energy balance monitoring in the Australian Murray-Darling Basin using GCOM-W1 data’. During JFY 2018, this project focused on: i) validation of the low resolution AMSR2 soil moisture products and ii) a high resolution downscaled AMSR2 soil moisture product. Similar as JFY 2017, results indicated that the AMSR2 L3 soil moisture product match with the JAXA tower and in-situ station measurements relatively well during the dry season when soil moisture is smaller than $0.1 \text{ m}^3/\text{m}^3$). However, during the wet season (soil moisture ranges from $0.1\text{-}0.5 \text{ m}^3/\text{m}^3$), the AMSR2 product tends to underestimate the condition by around $0.1\text{-}0.3 \text{ m}^3/\text{m}^3$ compared with the peak soil moisture values. Nevertheless, the underestimation status is better than the wetter years 2015-2016. It is suggested that the AMSR2 L3 soil moisture algorithm needs to be improved in the future. The downscaling schemes and the soil moisture retrieval algorithms were also presented in this report. Results show the relationship between downscaled C-band TB and airborne L-band TB observations align very well with the low-resolution SMAP L-band TB against AMSR2 C-band TB. Research on soil moisture retrieval from the downscaled C-band TB is currently underway. The results will be included in the paper manuscript scheduled to be drafted in mid-2019 as well as in future progress report.

References

- De Jeu, R. A. M., Holmes, T. R. H., Parinussa, R. M. & Owe, M. (2014). A spatially coherent global soil moisture product with improved temporal resolution. *Journal of Hydrology*, 516: 284-296.
- Gevaert, A. I., Parinussa, R. M., Renzullo, L. J., Van Dijk, A. I. J. M. and De Jeu, R. A. M. (2015). Spatio-temporal evaluation of resolution enhancement for passive microwave soil moisture and vegetation optical depth. *International Journal of Applied Earth Observation and Geoinformation*.
- Liu, J.G., 2000. Smoothing filter-based intensity modulation: a spectral preserve image fusion technique for improving spatial details. *Int. J. Remote Sens.* 21(18), 3461–3472, <http://dx.doi.org/10.1080/014311600750037499>.
- McKenzie, N.J., D.W. Jacquier, L.J. Ashton and H.P. Cresswell (2000), “Estimation of soil properties using the Atlas of Australian Soils,” *CSIRO Land and Water Technical Report 11/00*.
- Parinussa, R. M., Yilmaz, M. T., Anderson, M. C., Hain, C. R. & De Jeu, R. A. M. (2014) An intercomparison of remotely sensed soil moisture products at various spatial scales over the Iberian Peninsula. *Hydrological Processes*, 28: 4865-4876.
- Rudiger, C., Walker, J.P., Kerr, Y.H. (2011) On The Airborne Spatial Coverage Requirement for Microwave Satellite Validation. *IEEE Geoscience and Remote Sensing Letters*, 8(4):824-828. doi:10.1109/LGRS.2011.2116766.

- Santi, E. (2010). An application of the SFIM technique to enhance the spatial resolution of spaceborne microwave radiometers. *International Journal of Remote Sensing*, 31: 2419-2428.
- T. Mo, B. J. Choudhury, T. J. Schmugge, J. R. Wang, T. J. Jackson, "A model for the microwave emission of vegetation-covered fields", *J. Geophys. Res.*, vol. 87, no. 11, pp. 229-237, Dec. 1982.
- Yee, M., Walker, J. P., Monerris, A., Rudiger, C. and Jackson, T. J. (2016). On the identification of representative in situ soil moisture monitoring stations for the validation of SMAP soil moisture products in Australia. *Journal of Hydrology*, 537,, 367-381. doi:10.1016/j.jhydrol.2016.03.060
- Yee, M., Walker, J. P., Rüdiger, C., Robert M. Parinussa, Kerr, Y. and Koike, T. (2016). A comparison of SMOS and AMSR2 soil moisture using representative sites of the OzNet monitoring network. *Remote Sensing of Environment*. Manuscript in review.

**Validation of global water and energy
balance monitoring in the Australian
Murray-Darling Basin using GCOM-W1
data**
